The Na^+-dependent chloride-bicarbonate exchanger SLC4A8 mediates an electroneutral Na^+ reabsorption process in the renal cortical collecting ducts of mice

Françoise Leviel,[1,2,3] Christian A. Hübner,[4,5] Pascal Houillier,[1,2,3] Luciana Morla,[1] Soumaya El Moghrabi,[1] Gaëlle Brideau,[1] Hassan Hatim,[6] Mark D. Parker,[7] Ingo Kurth,[5] Alexandra Kougioumtzes,[5] Anne Sinning,[4] Vladimir Pech,[8] Kent A. Riemondy,[9] R. Lance Miller,[9] Edith Hummler,[10] Gary E. Shull,[11] Peter S. Aronson,[6] Alain Doucet,[1] Susan M. Wall,[8] Régine Chambrey,[1] and Dominique Eladari[1,2,3]

[1]Centre de recherche des Cordeliers, Université Pierre et Marie Curie, ERL CNRS 7226, INSERM UMRS 872 (Equipe 3), Paris, France. [2]Département de Physiologie, HEGP-Necker-Enfants Malades, AP-HP, Paris, France. [3]Faculté de Médecine Paris Descartes, Université Paris Descartes, Paris, France. [4]Institute for Clinical Chemistry, University Hospital Jena, Friedrich Schiller Universität, Jena, Germany. [5]Department of Human Genetics, Universitätsklinikum Hamburg-Eppendorf, Hamburg, Germany. [6]Yale University School of Medicine, Department of Internal Medicine, Section of Nephrology, New Haven, Connecticut, USA. [7]Case Western Reserve University School of Medicine, Cleveland, Ohio, USA. [8]Emory University School of Medicine, Department of Medicine, Renal Division, Atlanta, Georgia, USA. [9]Department of Pediatrics, Division of Nephrology, University of Utah, Salt Lake City, Utah, USA. [10]Université de Lausanne, Département de Pharmacologie et de Toxicologie, Lausanne, Switzerland. [11]University of Cincinnati, Department of Molecular Genetics, Cincinnati, Ohio, USA.

Regulation of sodium balance is a critical factor in the maintenance of euvolemia, and dysregulation of renal sodium excretion results in disorders of altered intravascular volume, such as hypertension. The amiloride-sensitive epithelial sodium channel (ENaC) is thought to be the only mechanism for sodium transport in the cortical collecting duct (CCD) of the kidney. However, it has been found that much of the sodium absorption in the CCD is actually amiloride insensitive and sensitive to thiazide diuretics, which also block the Na-Cl cotransporter (NCC) located in the distal convoluted tubule. In this study, we have demonstrated the presence of electroneutral, amiloride-resistant, thiazide-sensitive, transepithelial NaCl absorption in mouse CCDs, which persists even with genetic disruption of ENaC. Furthermore, hydrochlorothiazide (HCTZ) increased excretion of Na^+ and Cl^- in mice devoid of the thiazide target NCC, suggesting that an additional mechanism might account for this effect. Studies on isolated CCDs suggested that the parallel action of the Na^+-driven Cl^-/HCO_3^- exchanger (NDCBE/SLC4A8) and the Na^+-independent Cl^-/HCO_3^- exchanger (pendrin/SLC26A4) accounted for the electroneutral thiazide-sensitive sodium transport. Furthermore, genetic ablation of SLC4A8 abolished thiazide-sensitive NaCl transport in the CCD. These studies establish what we believe to be a novel role for NDCBE in mediating substantial Na^+ reabsorption in the CCD and suggest a role for this transporter in the regulation of fluid homeostasis in mice.

Introduction

Sodium chloride is the main extracellular osmotic constituent and thereby determines extracellular volume and blood pressure. To maintain a constant extracellular volume, the kidney has to match sodium excretion to dietary sodium intake. Abnormal retention of sodium by the kidney can ultimately lead to expansion of the extracellular volume and hypertension (1), the most common pathological state in humans. Since sodium is freely filtered by the glomerulus, most of it has to be reabsorbed as the filtrate flows along the nephron. This reabsorption is mediated by the Na^+/H^+ exchanger NHE3 in the proximal tubule (2), by the $Na^+/K^+/2Cl^-$ cotransporter NKCC2 in the thick ascending limb of Henle's loop (3), and by the NaCl cotransporter NCC in the distal convoluted tubule (DCT) (3, 4). Finally, the remaining fraction of filtered sodium enters the connecting tubule and the collecting duct. In these latter segments, aldosterone increases distal sodium reabsorption via the Na^+ channel ENaC (5). Supporting the importance of renal Na^+ handling in blood pressure regulation, inactivating mutations in the genes that code for renal sodium transporters are associated with low blood pressure (6–10), whereas inherited and acquired forms of hypertension can result from increased renal sodium reabsorption (11).

Drugs that selectively block the different aforementioned renal sodium transporters are the pharmacological basis of treatment of disease states characterized by abnormal renal sodium retention, such as edematous disorders and hypertension. Although discovered half a century ago (12), thiazides have been the cornerstone of therapy for mild and moderate hypertension in nearly all prospective therapeutic trials to date (13). Their efficacy in preventing hypertensive cardiovascular complications such as stroke and congestive heart failure has been verified in large clinical trials (14). Thiazides are believed to act exclusively by blocking sodium absorption via NCC, which represents only approximately 5%

Authorship note: Françoise Leviel and Christian A. Hübner share first authorship. Pascal Houillier and Luciana Morla contributed equally to this work.

Conflict of interest: The authors have declared that no conflict of interest exists.

Citation for this article: *J Clin Invest.* 2010;120(5):1627–1635. doi:10.1172/JCI40145.

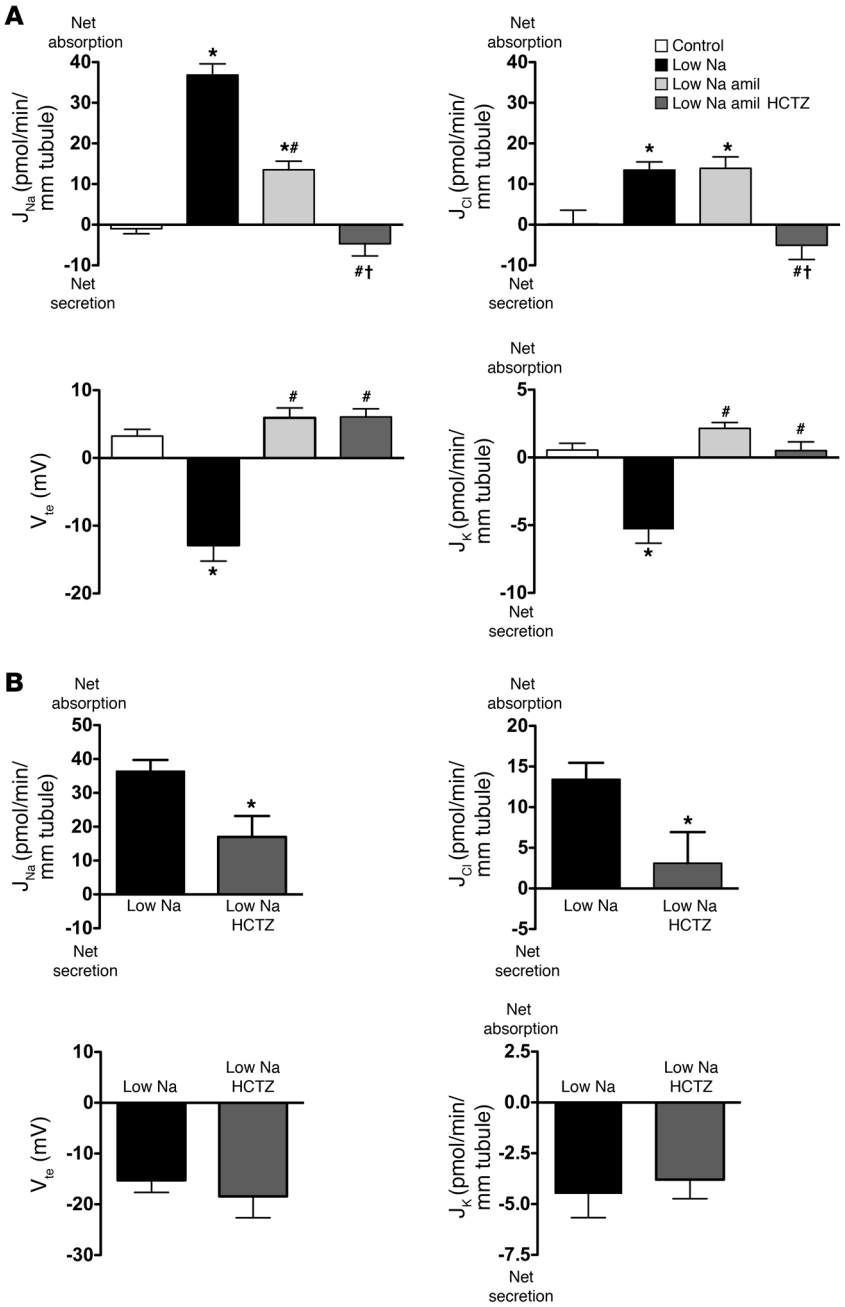

Figure 1

Pharmacological characterization of transepithelial transport of Na^+, K^+, and Cl^- in collecting ducts isolated from wild-type mice. (**A**) Effects of amiloride (10^{-5} M) and HCTZ (10^{-4} M) on Na^+, Cl^-, and K^+ transepithelial fluxes and on transepithelial voltage in CCDs isolated from Na^+-restricted mice. J_{Na}, rate of Na^+ absorption; J_{Cl}, rate of Cl^- absorption; V_{te}, transepithelial voltage; J_K, rate of K^+ secretion. Statistical significance was assessed by ANOVA; comparisons between groups were tested by Bonferroni's post-hoc test. $n = 5$ in each group, $^*P < 0.05$ versus control, $^{\#}P < 0.05$ versus low Na^+; $^{\dagger}P < 0.05$ versus low Na^+ amiloride (amil). (**B**) Effects of HCTZ alone (10^{-4} M) on Na^+, Cl^-, and K^+ transepithelial fluxes and on transepithelial voltage in CCDs isolated from Na^+-restricted mice. Statistical significance was assessed by 2-tailed unpaired Student's *t* test. $n = 5$ in each group; $^*P < 0.05$ versus control (low Na).

of the total amount of Na^+ filtered by the glomerulus (15, 16). However, previous studies have shown that approximately 50% of Na^+ absorption in the rat collecting duct is thiazide sensitive and amiloride insensitive (17–19), even though the expression of its canonical target, NCC, is restricted to the DCT.

Given its clinical relevance, we aimed to identify the transport system that accounts for this amiloride-insensitive, thiazide-sensitive Na^+ absorption in the cortical collecting duct (CCD). With a combined functional and genetic approach, we show that the parallel action of the Na^+-independent anion exchanger pendrin/Pds/SLC26A4 and the Na^+-dependent anion exchanger NDCBE/SLC4A8 mediates thiazide-sensitive electroneutral NaCl reabsorption in the CCD. This finding may have important implications for the treatment of arterial hypertension and our understanding of the role of the CCD in the regulation of Na^+ and K^+ homeostasis.

Results

Electrogenic and electroneutral Na^+ absorption pathways coexist in the mouse collecting duct. To verify the presence of the previously reported thiazide-sensitive component of Na^+ absorption, we simultaneously measured transepithelial Na^+ (J_{Na}), K^+ (J_K), and Cl^- (J_{Cl}) fluxes and transepithelial voltage (V_{te}) in isolated mouse CCDs microperfused in vitro. Because mouse CCDs do not absorb NaCl under basal conditions (see ref. 20 and control group in Figure 1A), we stimulated NaCl absorption by feeding the mice a Na^+-depleted diet for 2 weeks before the experiments. CCDs from NaCl-restricted wild-type mice absorbed Na^+ and Cl^-, secreted K^+, and generated a lumen-negative transepithelial voltage (V_{te}), consistent with ENaC-mediated Na^+ absorption (Figure 1A). Amiloride in the perfusate, at concentrations that fully inhibit ENaC (10^{-5} M) (21), did not change Cl^- absorption (Figure 1A), although both V_{te} and K^+ secretion were eliminated and Na^+ absorption was reduced by 60% (Figure 1A). In contrast, luminal addition of 10^{-4} M hydrochlorothiazide (HCTZ) abolished both J_{Cl} and the amiloride-insensitive component of J_{Na}, whereas J_K and V_{te} were not affected by HCTZ (Figure 1A). We next tested the effects of luminal addition of 10^{-4} M HCTZ on J_{Na}, J_{Cl}, J_K, and V_{te} in the absence of amiloride. Figure 1B shows that HCTZ decreased Na^+ absorption by approximately 45% and almost abolished Cl^- absorption. However, HCTZ did not affect either V_{te} or K^+ secretion (Figure 1B). Taken together, these results strongly support the hypothesis that HCTZ inhibits a system that is different from ENaC and that mediates electroneutral NaCl absorption in the mouse collecting duct.

To further exclude a role for ENaC in the amiloride-insensitive, HCTZ-sensitive component of sodium reabsorption, we similarly

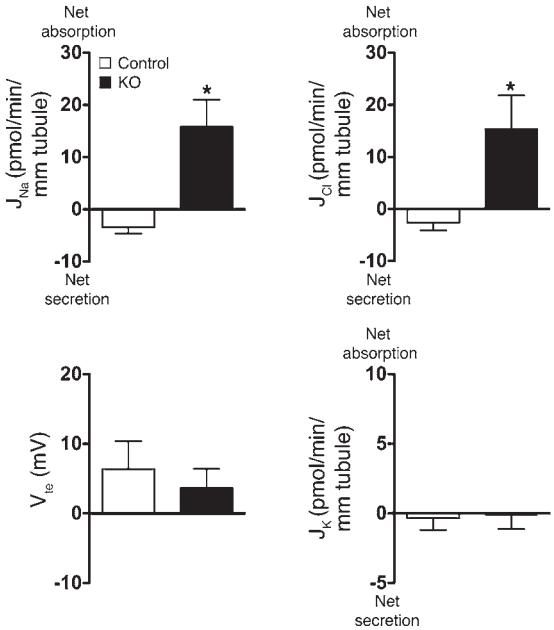

Figure 2
Analyses of J_{Na}, J_{Cl}, and J_K and V_{te} in CCDs isolated from collecting duct–specific ENaC–KO mice maintained on a Na^+-depleted diet. The control group consists of littermate mice floxed for α-ENaC but negative for the HoxB7-Cre transgene, as detailed elsewhere (22). The control group was kept on a normal Na^+ diet to provide the zero baseline values for each variable. Statistical significance was assessed by 2-tailed unpaired Student's *t* test. $n = 5$ in each group; $^*P < 0.05$.

studied isolated perfused CCDs from mice with a collecting duct–specific disruption of α-ENaC (22) in vitro. It has been shown previously in this genetic model that disruption of the *Scnn1a* locus in the CCD abolishes α-ENaC protein expression and prevents the apical membrane expression of β and γ subunits in CCD cells (22), resulting in the complete ablation of ENaC channel activity in the collecting duct (22). As shown in Figure 2, CCDs from control mice on a normal Na^+ diet again had no significant Na^+, Cl^-, or K^+ transport. Importantly, as also shown in Figure 2, CCDs from collecting duct–specific ENaC–KO mice on a Na^+-depleted diet absorbed Na^+ and Cl^- but did not generate a lumen-negative transepithelial voltage and did not secrete K^+. Our results confirm that the thiazide-sensitive component of Na^+ absorption is ENaC independent and most likely occurs through an electroneutral mechanism that does not promote K^+ secretion.

CCDs from NCC-deficient mice display thiazide-sensitive NaCl absorption. To investigate whether the thiazide-sensitive component of Na^+ absorption in the CCD might occur through NCC, we measured ion transport and V_{te} in CCDs from mice with a genetic disruption of *Slc12a3*, the gene encoding NCC (*Ncc*$^{-/-}$ mice) (23). Western blot and immunofluorescence analyses confirmed the complete absence of the NCC protein in this mouse model (24, 25). CCDs from *Ncc*$^{-/-}$ mice on a NaCl-replete diet absorbed Na^+ and Cl^-, whereas CCDs from pair-fed wild-type mice did not (Figure 3). Thus, after genetic disruption of *Slc12a3*, NaCl absorption was increased in the CCD, presumably consequent to sodium depletion. NaCl absorption in CCDs from *Ncc*$^{-/-}$ mice was amiloride insensitive but was fully inhibited by HCTZ (Figure 3). A lumen-negative V_{te} or K^+ secretion in CCDs from *Ncc*$^{-/-}$ mice was never observed in any of the experimental conditions studied (data not shown). Thus, under NaCl-replete conditions, CCDs from mice with a targeted disruption of *Ncc* have little ENaC-mediated Na^+ absorption but have robust electroneutral, thiazide-sensitive NaCl reabsorption.

To assess the physiological relevance of this transport system, we investigated whether thiazides have a diuretic effect in vivo in the absence of NCC (Figure 4). Consistent with the in vitro studies, we observed significant HCTZ-induced natriuresis and chloriuresis in *Ncc*$^{-/-}$ mice, although the response was smaller and delayed relative to that in *Ncc*$^{+/+}$ mice (Figure 4). We conclude that NCC-independent thiazide-sensitive sodium absorption participates in renal sodium absorption and regulation of sodium balance in vivo.

Thiazide-sensitive NaCl absorption in the CCD is bicarbonate dependent and involves 2 ion transporters. In many epithelia, NaCl transport occurs through a Cl^-/HCO_3^- and a Na^+/H^+ exchanger working in parallel. In the CCD, Cl^- absorption is eliminated with genetic ablation of *Slc26a4* (20, 26), the gene encoding the Cl^-/HCO_3^- exchanger pendrin that is found in the apical regions of type B and non-A–non-B intercalated cells (27). Since Cl^- transport in the CCD occurs through pendrin, we hypothesized that HCTZ-sensitive NaCl transport results from the coupling of pendrin-mediated Cl^- reabsorption with H^+/HCO_3^--dependent Na^+ transport. Supporting this hypothesis, removal of CO_2/HCO_3^- from the perfusion and bath solutions abolished both Na^+ and Cl^- transport by perfused CCDs isolated from *Ncc*$^{-/-}$ mice (Figure 5).

To identify the apical sodium transporter, we measured changes in intracellular pH (pH_i) in response to luminal Na^+ removal and then to luminal Na^+ readdition. Experiments were performed in the absence of basolateral Na^+ to silence basolateral Na^+/H^+ exchange. Intercalated cells were distinguished from principal cells by their fluorescein-conjugated peanut lectin labeling (28) and by their greater uptake of BCECF when the fluorophore was added

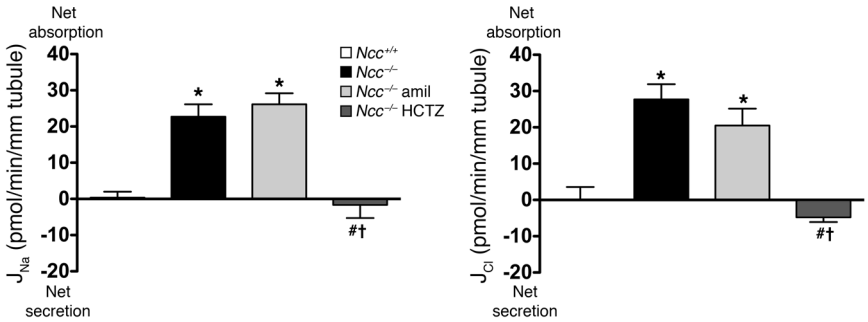

Figure 3
Effects of amiloride (10^{-5} M) and HCTZ (10^{-4} M) on Na^+ and Cl^- transepithelial fluxes in CCDs isolated from *Ncc*$^{+/+}$ and *Ncc*$^{-/-}$ mice fed a Na^+-replete diet. Statistical significance was assessed by ANOVA; comparisons between groups were tested by Bonferroni's post-hoc test. $n = 5$ in each group; $^*P < 0.05$ versus *Ncc*$^{+/+}$; $^{\#}P < 0.05$ versus *Ncc*$^{-/-}$; $^{\dagger}P < 0.05$ versus *Ncc*$^{-/-}$ amil.

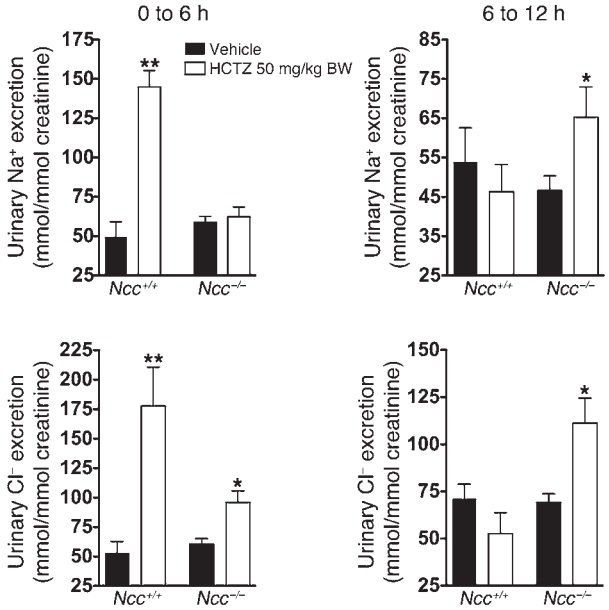

Figure 4
Effects of HCTZ on urinary excretion of Na^+ and Cl^- in *Ncc*$^{+/+}$ and *Ncc*$^{-/-}$ mice. One single dose of HCTZ (50 mg/kg body weight) or vehicle was administered intraperitoneally to *Ncc*$^{+/+}$ and *Ncc*$^{-/-}$ mice. Urine samples were collected from 0 to 6 and from 6 to 12 hours after injection to measure urinary Na^+ (top panels) or Cl^- (bottom panels) excretion. Results are expressed as the ratio to urinary creatinine. Statistical significance was assessed by 2-tailed Student's unpaired *t* test. $n = 5$ in WT groups and $n = 8$ in KO groups; $^*P < 0.05$, $^{**}P < 0.01$ versus vehicle.

to the perfusate (29). Whereas in CCDs isolated from wild-type mice fed a standard Na^+-replete diet, pH_i in both intercalated and principal cells was insensitive to changes in luminal Na^+ (data not shown), and intercalated cell pH_i in CCDs of Na^+-depleted wild-type mice fell with removal of Na^+ from the perfusate. This drop in pH_i was fully reversed when Na^+ was reintroduced into the lumen (Figure 6A). These findings indicate the presence of a Na^+-coupled acid-base transporter that is upregulated in the apical membrane of intercalated cells in response to a Na^+-restricted diet. Furthermore, the activity of this transporter was abolished in the absence of Cl^- and greatly reduced in the nominal absence of CO_2/HCO_3^- (Figure 6A), indicating that sodium uptake is mediated by a Na^+-driven Cl^-/HCO_3^- exchanger rather than by a Na^+/H^+ exchanger or a Na^+-HCO_3^- cotransporter. Because luminal removal of Na^+ did not elicit any detectable pH_i changes in principal cells in the CCD (data not shown), this Na^+-driven Cl^-/HCO_3^- exchanger appears to be restricted to intercalated cells.

While many HCO_3^- transporters have been reported in the mammalian kidney, only NDCBE (encoded by *Slc4a8*) mediates Na^+- and Cl^--dependent HCO_3^- transport (30, 31). NDCBE promotes the electroneutral exchange of 1 intracellular Cl^- ion for 1 Na^+ and 2 HCO_3^- ions. Although predominantly expressed in the brain and testis, NDCBE is also detected in the kidney, the digestive tract, the retina, the thyroid, the aorta, and the spinal cord (see Supplemental Figure 1A and Supplemental Figure 2; supplemental material available online with this article; doi:10.1172/JCI40145DS1). *Slc4a8* transcripts were confirmed in mouse CCDs by RT-PCR (data not shown). Since our preceding experiments suggested that NDCBE might be important for Na^+ transport by intercalated cells, we genetically disrupted *Slc4a8* in mice (Supplemental Figure 1, B and C). *Ndcbe*$^{-/-}$ mice produced from heterozygous matings followed Mendelian ratios and had no obvious phenotypical abnormalities. NDCBE protein was detected by immunoblot in renal cortex and isolated CCDs of wild-type mice, but not in *Ndcbe*$^{-/-}$ mice (Figure 6B).

To determine whether NDCBE participates in amiloride-resistant NaCl transport in mouse CCDs, we characterized Na^+ and Cl^- transport in CCDs from *Ndcbe*$^{-/-}$ mice. Whereas amiloride-resistant NaCl absorption was detectable in CCDs from Na^+-depleted WT mice, NaCl absorption in the presence of luminal amiloride was not different from zero in CCDs from Na^+ depleted *Ndcbe*$^{-/-}$ mice, demonstrating that amiloride-resistant Na^+ transport depends on NDCBE (Figure 6C).

To assess whether HCTZ inhibits amiloride-resistant NaCl absorption by blocking NDCBE, and/or pendrin, we next tested the effects of 10^{-4} M HCTZ on Na^+-dependent and Na^+-independent Cl^-/HCO_3^- exchange activities. Na^+-dependent pH changes, in the nominal presence of extracellular Cl^- and HCO_3^-, were present in CCDs of Na^+-depleted *Ndcbe*$^{+/+}$ mice but completely abolished in CCDs of Na^+-depleted *Ndcbe*$^{-/-}$ mice (Figure 7A), confirming the role of NDCBE in mediating this process. In addition, Na^+-dependent pH_i changes were abolished by luminal HCTZ (10^{-4} M). Similarly, apical Cl^-/HCO_3^- exchange mediated by pendrin was abolished by luminal HCTZ (Figure 7B). However, when heterologously expressed in *Xenopus* oocytes, NDCBE activity was not significantly affected by HCTZ (0.25 mM), and pendrin activity was inhibited by HCTZ (Figure 7C), although inhibition was only partial and required higher (1 mM) HCTZ concentrations than those found to inhibit this process in isolated CCDs. This difference in sensitivity could be due to the very different experimental conditions (e.g., temperature of the assays). However, it is also possible that HCTZ has an additional indirect effect of inhibiting NDCBE or pendrin in native CCDs. As HCTZ does not block NCC exclusively, but also inhibits carbonic anhydrase (32), we next tested the effects of the carbonic anhydrase inhibitor acetazolamide (ACZ) on J_{Na} and J_{Cl} and on NDCBE and pendrin activities measured in isolated CCDs. While ACZ abolished Cl^- absorption (Figure 8A) as well as Na^+-independent Cl^-/HCO_3^- exchange (i.e., pendrin) activity (Figure 8B), it had no effect on Na^+ absorption (Figure 8C) or on NDCBE activity (Figure 8D),

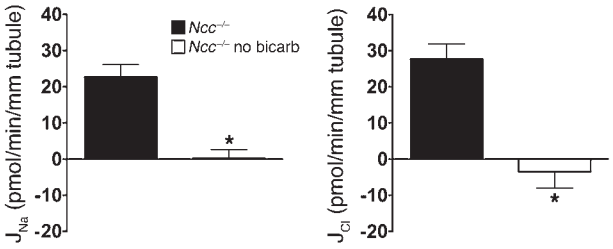

Figure 5
Effects of bicarbonate on transepithelial fluxes of Na^+ and Cl^- in CCDs isolated from *Ncc*$^{-/-}$ mice. CCDs from *Ncc*$^{-/-}$ mice were either perfused in CO_2/HCO_3^--containing solutions or in CO_2/HCO_3^--free (no bicarbonate [no bicarb]) buffer. Statistical significance was assessed by 2-tailed Student's unpaired *t* test. $n = 5$ in each group; $^*P < 0.001$ versus control.

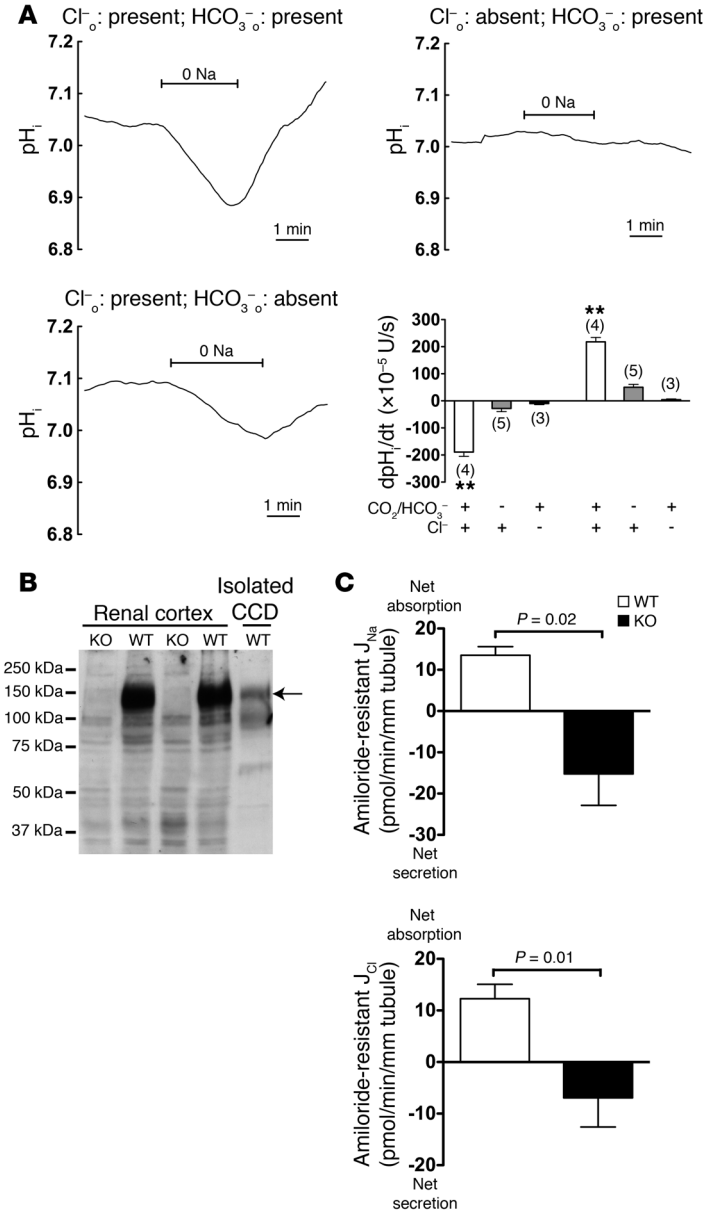

Figure 6

Detection and functional characterization of NDCBE in collecting ducts isolated from wild-type mice fed a Na^+-depleted diet. (**A**) Na^+ dependence of pH_i changes in intercalated cells of CCDs isolated from mice fed a Na^+-depleted diet. Traces are the average of pH_i changes recorded when luminal Na^+ was removed from, and then readded to the perfusate. Upper-left panel: Both Cl^- and HCO_3^-/CO_2 were present in the extracellular fluid; mean starting pH_i (immediately before luminal Na^+ removal) was 7.03 ± 0.04. Upper right: extracellular Cl^- was absent; mean starting pH_i was 7.03 ± 0.05. Lower left: extracellular HCO_3^-/CO_2 was absent; mean starting pH_i was 7.09 ± 0.11. Lower right: initial rates of pH_i changes during exposure to different solutions. Values are mean ± SEM, with number of tubules in parentheses. Statistical significance was tested by ANOVA followed by Bonferroni's post-hoc test. $^{**}P < 0.01$ versus all other groups. o, outside. (**B**) Western blot analyses of NDCBE in the mouse kidney and CCD. Western blot analyses of 50 μg membrane fraction proteins from renal cortex isolated from *Ndcbe*$^{-/-}$ mice or wild-type mice or of proteins from 100 CCDs (corresponding to ~25 mm of tubule) isolated from wild-type mice. NDCBE was detected in the renal cortex or isolated tubules of wild-type but not of *Ndcbe* $^{-/-}$ mice. Note that the apparent difference in abundance of NDCBE between the lane loaded with total cortex and the one loaded with isolated CCD does not reflect an enrichment of the cortex versus the CCD, but actually only reflects the difference in the quantity of protein loaded. (**C**) Analyses of amiloride-resistant Na^+ and Cl^- transepithelial fluxes in CCDs isolated from NDCBE-KO mice maintained on a Na^+-depleted diet. Fluxes were measured in the presence of 10^{-5} M amiloride in the perfusate to reflect only the amiloride-resistant, HCTZ-sensitive component of NaCl reabsorption. Values are mean ± SEM; statistical significance was assessed by unpaired Student's *t* test with Welch's correction, when appropriate. $n = 5$ in each group.

which excludes the possibility that HCTZ affects Na^+ transport through its effect on carbonic anhydrase.

Taken together, these data confirm that HCTZ inhibits NDCBE and pendrin in the intact tubule and thereby amiloride-resistant electroneutral NaCl absorption in the CCD.

Discussion

Only two apical sodium transporters are established in the distal nephron where aldosterone modulates sodium, potassium, and acid-base homeostasis: the thiazide-sensitive cotransporter NCC (4), which mediates electroneutral NaCl cotransport, and the amiloride-sensitive sodium channel ENaC (5), which mediates electrogenic Na^+ absorption (Recently, the Na^+-HCO_3^- cotransporter NBCn1/Slc4a7 has also been shown to be present in the collecting duct [refs. 33, 34]. However, no evidence has been reported yet that NBCn1 participates in transepithelial Na^+ absorption.) Except at the very end of the DCT (or DCT2), there is no overlap of expression of the 2 proteins, as NCC is restricted to the DCT and ENaC to principal cells of the connecting tubule and collecting duct, respectively (35). Here, we identified what we believe to be a new mechanism of apical NaCl uptake in the collecting duct that results from parallel operation of 2 bicarbonate transporters: the Na^+ driven Cl^-/HCO_3^- exchanger NDCBE and the Na^+-independent anion exchanger pendrin. In vivo and in isolated tubules, this mechanism mediates net electroneutral thiazide-sensitive NaCl reabsorption in the CCD, thereby exhibiting an "NCC-like" activity. Our findings explain why thiazides block 50% of sodium absorption in rat CCD (17–19), although NCC was repeatedly shown to be absent from this nephron segment in different species (36–39). Moreover, the demonstration of thiazide-sensitive NaCl absorption in mice with genetic ablation of NCC (Figure 3) definitively rules out a possible involvement of the latter in this

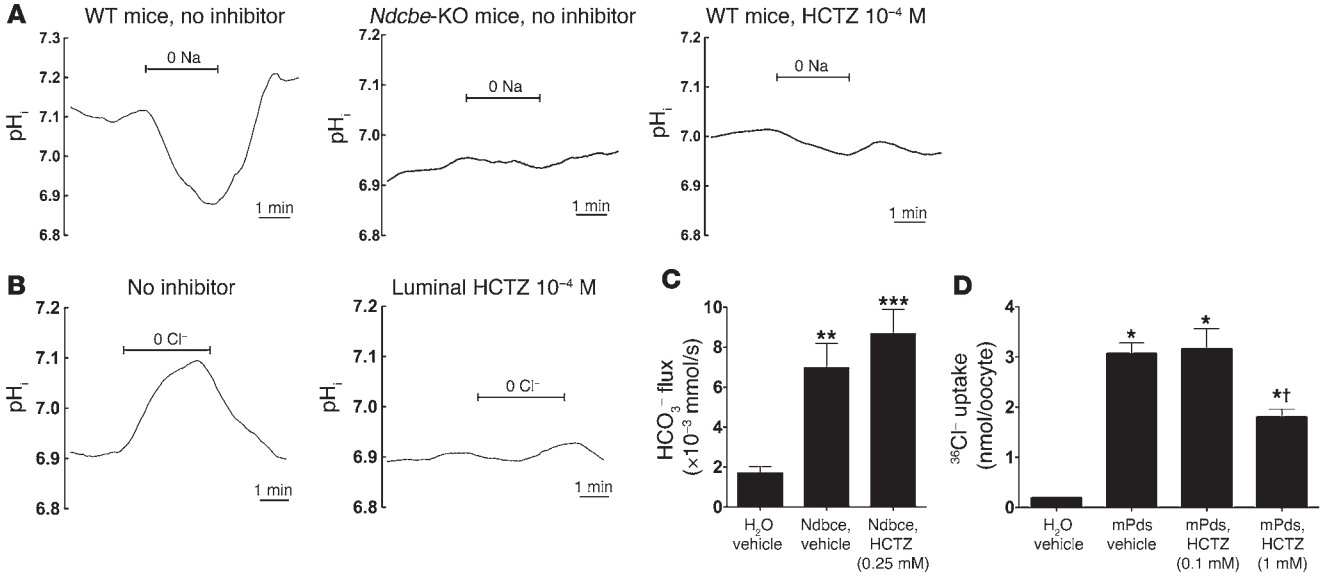

Figure 7

Effects of HCTZ (10^{-4} M) on NDCBE or PDS activity in isolated collecting ducts or on recombinant NDCBE or PDS expressed in *Xenopus* oocytes. (**A**) Effects of HCTZ and *Ndcbe* disruption on Na^+-dependent pH_i changes measured in intercalated cells of CCD isolated from Na-depleted *Ndcbe*$^{-/-}$ or *Ndcbe*$^{+/+}$ mice fed a low-Na^+ diet. Traces are the average of pH_i changes recorded when luminal Na^+ was removed and then readded, in the presence of extracellular Cl^- (122 mM) and HCO_3^- (25 mM). Intracellular Na^+-dependent acidification was detected in *Ndcbe*$^{+/+}$ mice but absent in *Ndcbe*$^{-/-}$ mice or when HCTZ 10^{-4} M was present in the perfusate. In these 3 different experimental conditions, mean starting pH_i values were 7.10 ± 0.02, 6.93 ± 0.11, and 7.01 ± 0.04, respectively. (**B**) Effects of HCTZ on apical Cl^-/HCO_3^- exchange activity in intercalated cells of CCDs isolated from Na-depleted animals. Traces are the average of pH_i changes recorded when luminal Cl^- was removed and then readded, in the presence of extracellular HCO_3^- (25 mM) and in Na^+-free solutions. Intracellular Cl^--dependent alkalinization, reflecting apical Cl^-/HCO_3^- exchange, was completely abolished when 10^{-4} M HCTZ was present in the perfusate. Mean starting pH_i values (immediately before Cl^- removal) were 6.91 ± 0.03 and 6.89 ± 0.08, in the absence and presence of HCTZ, respectively. (**C**) Effects of HCTZ on mNdcbe-mediated HCO_3^- influx. Oocytes had been injected with mNdcbe cRNA or H_2O and incubated with HCTZ (0.25 mM). As a control, NDCBE-expressing and H_2O-injected oocytes were incubated with vehicle (methanol). Values are mean ± SEM with 6–9 oocytes per group. $^{**}P < 0.01$, $^{***}P < 0.001$ versus H_2O-injected oocyte. HCO_3^- flux was unaffected by the application of HCTZ (0.25 mM) compared with vehicle alone ($P = 0.279$). (**D**) Effects of HCTZ on Pds-mediated $^{36}Cl^-$ uptake. Pendrin-expressing oocytes (mPds) were incubated in ND96 containing 0.1 or 1 mM HCTZ during the uptake period (16 minutes). As a control, pendrin-expressing and H_2O-injected oocytes were incubated with vehicle (methanol). Values are mean ± SEM, with 6–16 oocytes per group. $^*P < 0.001$ versus H_2O; $^\dagger P < 0.001$ versus mPds, HCTZ 0.1 mM.

process. It is likely that the Na^+ reabsorption pathway we describe here plays a relevant role in the regulation of sodium balance, since it is stimulated in response to either dietary sodium restriction (Figure 1) or renal salt wasting upon disruption of NCC (Figure 3); moreover, its inhibition by HCTZ increases Na^+ and Cl^- excretion in NCC-deficient mice (Figure 4). Thus, our data imply that the anti-hypertensive action of thiazides might be, at least partially, mediated by inhibition of sodium transport in the CCD and not exclusively in the DCT. The observations that mice with impaired expression of ENaC all along the distal nephron exhibit marked renal salt wasting, mimicking pseudohypoaldosteronism type I (PHA1) (40), whereas mice with collecting duct–specific ablation of ENaC maintain sodium balance even when challenged with a low-sodium diet (22), have suggested that the collecting duct does not importantly participate in the regulation of extracellular volume, since increased ENaC activity and expression in the late DCT and the CNT are able to fully compensate for ENaC deletion in the CCD (22, 41). However, the present finding that collecting ducts isolated from these mice exhibit net electroneutral NaCl absorption after sodium deprivation also supports the concept that ENaC is not the only important mechanism responsible for adaptive changes of sodium absorption in the collecting duct. Indeed, based on our results, it is possible that NDCBE/pendrin might also represent part of the compensatory mechanism. Nevertheless, the observation that complete ENaC deletion leads to PHA1 indicates that electroneutral NaCl absorption through the intercalated cells cannot fully replace ENaC-mediated Na^+ absorption but rather plays a complementary role.

Within the distal nephron, sodium transport is important not only for sodium balance regulation but also for potassium and acid-base homeostasis. In fact, sodium absorption through ENaC in principal cells is electrogenic and generates a lumen-negative transepithelial voltage (Figure 1), which in turn stimulates K^+ and H^+ secretion. The importance of this mechanism is highlighted by the features of primary hyperaldosteronism, or Conn syndrome, in which the excess of aldosterone, the main hormone stimulating ENaC, promotes sodium retention and arterial hypertension together with renal hypokalemia and metabolic alkalosis. Conversely, blockade of ENaC, for example, by amiloride-related diuretics, leads to hyperkalemia and metabolic acidosis. However, under certain circumstances, such as dietary sodium restriction, which also stimulates aldosterone secretion, sodium balance is maintained by an increase in distal nephron sodium absorption without any alteration of K^+ or H^+ homeostasis (42). This phenom-

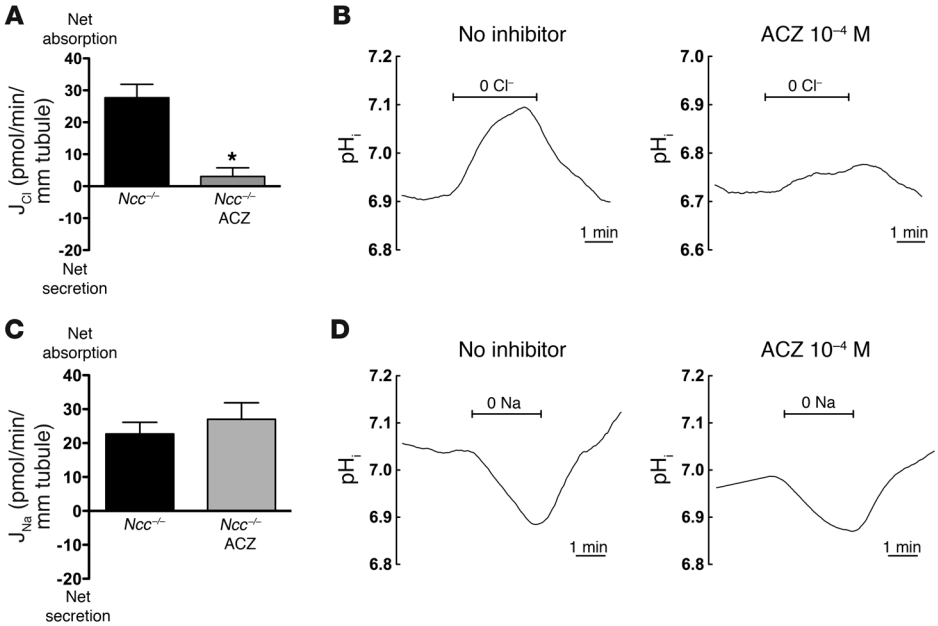

Figure 8

Effects of ACZ (10^{-4} M) on NDCBE- or PDS-dependent transport in isolated collecting ducts. (**A**) Effects of 10^{-4} M ACZ on Cl^- transepithelial transport in CCDs isolated from *Ncc*$^{-/-}$ mice. CCDs were isolated from *Ncc*$^{-/-}$ mice and bathed and perfused with CO_2/HCO_3^--containing solutions. Statistical significance was assessed by 2-tailed Student's unpaired *t* test. $n = 5$ in each group; $^*P < 0.001$ versus control. (**B**) Effects of luminal 10^{-4} M ACZ on pendrin activity in isolated CCDs. Tubules were isolated from wild-type mice. Pendrin activity was assessed by measuring changes in pH_i when Cl^- was removed and then readded from the perfusate. Both bath and perfusate solutions contained 25 mM HCO_3^- and were sodium-free. Traces represent the average of recordings from independent tubules. $n = 4$–5 independent tubules by group. Mean starting pH_i values were 6.91 ± 0.03 and 6.72 ± 0.05, in the absence and presence of ACZ, respectively. (**C**) Effects of luminal 10^{-4} M ACZ on Na^+ transepithelial transport in CCDs isolated from *Ncc*$^{-/-}$ mice. Statistical significance was assessed by 2-tailed Student's unpaired *t* test. $n = 5$ in each group. (**D**) Effects of ACZ 10^{-4} M on NDCBE activity in isolated CCDs. Tubules were isolated from wild-type mice. NDCBE activity was assessed by measuring changes in pH_i of intercalated cells when Na^+ was removed and then readded from the perfusate. Both bath and perfusate solutions contained 25 mM HCO_3^- and 122 mM Cl^-. The bath solution was sodium-free to silence basolateral Na^+/H^+ exchanger activity. Traces represent the average of recordings from independent tubules. $n = 4$–5 independent tubules by group. Mean starting pH_i values were 7.03 ± 0.04 and 6.99 ± 0.05, in the absence and presence of ACZ, respectively.

enon, known as the "aldosterone paradox," implies that, depending on the needs of the organism, the kidney is able to increase distal nephron sodium absorption with or without promoting K^+ or H^+ secretion. Recently, it was shown that the balance between electroneutral NaCl absorption by NCC within the DCT and electrogenic $Na^+/K^+(H^+)$ "exchange" promoted by ENaC in the connecting tubule and the collecting duct is finely tuned by the WNK pathway (43, 44). Our finding that the collecting duct also performs electroneutral NaCl absorption suggests that this balance might also occur within the CCD: The relative contribution of ENaC and pendrin/NDCBE to NaCl absorption in the CCD determines the magnitude of the transepithelial voltage in the CCD and thereby modulates K^+ and H^+ secretion. In the different situations studied here, electroneutral NaCl accounted for 40%–100% of total transepithelial Na^+ absorption. In *Ncc*$^{-/-}$ mice, a model in which upregulation of ENaC is thought to promote K^+ wasting (45), we observed that electroneutral NaCl transport was the dominant mechanism accounting for sodium absorption in the collecting duct. This suggests that *Ncc*$^{-/-}$ mice, by favoring this electroneutral pathway, are able to maintain NaCl balance while minimizing K^+ loss, as attested by the absence of overt hypokalemia in this model when dietary K^+ intake is maintained at a relatively high level (23, 45).

In summary, we have demonstrated what we believe to be a novel role of NDCBE in mediating ENaC-independent, thiazide-sensitive, and electroneutral Na^+ reabsorption in the CCD. This finding has important implications for understanding the action of thiazides on Na^+ reabsorption and blood pressure. Furthermore, the finding challenges the current concept of a functional separation between principal cells for the regulation of sodium and potassium balance and intercalated cells for acid-base regulation.

Methods

Animals. *Ncc*$^{-/-}$ and collecting duct–specific ENaC–KO mice have been characterized previously (22, 23). The generation of *Slc4a8*$^{-/-}$ mice is described below. Studies were performed in a pure C57BL/6 background for the Ncc strain and a mixed 129SV/C57BL/6 background for the other strains. The appropriate littermates were used as controls. All animal protocols were approved by the review board of the Centre de Recherche des Cordeliers, Paris, France.

Generation of Slc4a8-KO mice. A clone isolated from a 129/SvJ mouse genomic λ library (Stratagene) was used to construct the targeting vector. An approximately 11-kb *Eco*RI/*Kas*I fragment including exons 10–16 of the *Slc4a8* gene was cloned into the pKO-V901 plasmid (Lexicon Genetics) with a phosphoglycerate kinase (pgk) promoter–driven diphtheria toxin A cassette. A pgk promoter–driven neomycin resistance cassette flanked by loxP sites was inserted into the *Mfe*I site in intron 11. A third loxP site and an additional *Eco*RI site were inserted into the *Kpn*I site in intron 12. The construct was electroporated into R1 mouse embryonic stem cells. Neomycin-resistant clones were analyzed by Southern blot using *Eco*RI and an external approximately 500-bp probe. Correctly targeted ES cells were transfected with a plasmid expressing Cre-recombinase to remove the neomycin cassette and exon 12. Correctly recombined clones were identified with an internal second probe by Southern blot analysis after *Eco*RI digestion. Two independent embryonic stem cell clones were injected into C57BL/6 blastocysts to generate chimeras that were backcrossed with C57BL/6 mice. Studies were performed in a mixed 129Sv/C57BL/6 background in the F_6 and F_7 generation. Genotypes were determined either by Southern blot or by PCR of tail biopsy DNA. For PCR genotyping, the sense primers F1 (5′-GGCTAGGCAGTTCTTATCTTTCCC-3′), F2 (5′-GAGCAGCCCAGATGTACACCAGC-3′) and the antisense primers R1 (5′-GGCAATCCCCGTCATGGACG-3′) were used in a single PCR mix. The primer pair F1/R1 amplified a 320-bp wild-type allele, and the primer

pair F2/R1 a 423-bp KO allele. Southern and Northern blot analyses were performed as described in ref. 46.

Antibody generation and Western blot analysis. The NDCBE antiserum was raised in rabbits against the epitope ALSINSGNTKEKSPFN (amino acids 1,074–1,089, accession number NP_067505) and affinity purified. For Western blot analyses, 10–60 μg of the membrane-enriched protein fraction was separated on reducing 7.5% SDS-polyacrylamide gels. Blots were probed with the rabbit NDCBE antibody at a dilution of 1:250. Detection was done with the chemiluminescence ECL kit (Amersham Biosciences).

In vitro microperfusion, transepithelial ion fluxes, and pH measurements. CCD segments were isolated from corticomedullary rays under a dissecting microscope with a sharpened forceps. Because CCDs are highly heterogeneous, relatively short segments (0.45–0.6 mm) were dissected to maximize the reproducibility of the isolation procedure. In vitro microperfusion was performed as described by Burg et al. (47). Because CCDs from mice are frequently unstable and collapse rapidly, measurements were conducted during the first 90 minutes of perfusion. Usually, collections from 4 periods of 15 minutes were performed in which 15–20 nl of fluid were collected. The volume of the collections was determined under water-saturated mineral oil with calibrated volumetric pipettes. For [Na^+], [K^+], and [creatinine] measurements, 11–15 nl were required, while 2–3 nanoliters were used for [Cl^-] determinations. Transepithelial voltage (V_{te}) was measured continuously between Ag-AgCl electrodes connected to 0.15-M NaCl-agar bridges inserted in the perfusion pipette and bathing solutions. Values for each period were averaged.

Intracellular pH was monitored using the pH-sensitive dye BCECF (29). Intracellular dye was calibrated at the end of each experiment using the high-[K^+]/nigericin technique (48). Briefly, tubules were perfused and bathed with a HEPES-buffered, 95-mM K^+ solution containing 10 μM of the K^+/H^+ exchanger nigericin. Four different calibration solutions, titrated to 6.5, 6.9, 7.3, or 7.5, were used. V_{te} was measured continuously as described elsewhere (49). [Na^+], [K^+], and [creatinine] measurements were performed by HPLC (50). [Cl^-] was measured by microcoulometry (51). For each collection, ion flux (J) was calculated and reported to the length of the tubule: $J_{Na} = [([Na]_{perf} \times V_{perf}) - ([Na]_{coll} \times V_{coll})]/l$; $J_K = [([K]_{perf} \times V_{perf}) - ([K]_{coll} \times V_{coll})]/l$; and $J_{Cl} = [([Cl]_{perf} \times V_{perf}) - ([Cl]_{coll} \times V_{coll})]/l$, where "perf" indicates perfusate and "coll" indicates collection fluid.Therefore, positive values indicate net absorption, whereas negative values indicate net secretion of the ion. For each tubule, the mean of the 4 collection periods was used.

Measurement of pendrin and NDCBE activities in Xenopus oocytes. Full-length mouse pendrin and NDCBE cDNAs were cloned by PCR from isolated CCDs using the mouse pendrin-specific primers forward 5′-GTCATCCCTCGTCGCATC-3′ and reverse 5′-TCTCAGGAAGCAAGTCTACGC-3′; and the mouse NDCBE-specific primers forward 5′-CGCGGATCCGCCACCATGCCCGCCGGGAGCAA-3′ and reverse 5′-GCTCTAGATCAGTTGAAGGGGCTTTTTTCTTTTGTATTTCCGG-3′. Both PCR products were subsequently ligated into pGH19 (52) and linearized with *Xho*I. cRNAs were transcribed using T7 RNA polymerase (mMESSAGE mMACHINE), and their quality was assessed by spectroscopy and agarose gel electrophoresis.

Pendrin activity was assessed as pendrin-dependent ^{36}Cl uptake. Oocytes were prepared from *Xenopus laevis* as described previously (52). Briefly, stage V–VI oocytes were injected with 25 ng of pendrin cRNA and kept at 16–18°C in ND96 (in mM: 96.0 NaCl, 2.0 KCl, 1.0 $CaCl_2$, 1.8 $MgCl_2$, 5.0 HEPES, pH 7.4; supplemented with 5 mM sodium pyruvate and 50 U/ml penicillin/streptomycin) for 48 hours before measuring ^{36}Cl uptake. Oocytes were washed twice at room temperature in 1 ml chloride-free buffer (in mM: 98 potassium-gluconate, 1.8 hemi-calcium-gluconate, 1 hemi-magnesium-gluconate, 5 Tris-HEPES, pH 7.5) and then incubated in 500 μl uptake medium (in mM: 100 potassium-gluconate, 5 Tris, pH adjusted to 7.5 with HEPES) containing 1.74 mM ^{36}Cl for 16 minutes. The oocytes were then washed 3 times in ice-cold chloride-free buffer and subsequently lysed individually in 200 μl of 10% SDS. The radioisotope content of each individual oocyte was measured by scintillation spectrometry after adding 3 ml scintillation fluid (Opti-Fluor, Packard).

NDCBE activity was assessed as NDCBE-dependent bicarbonate influx as described previously (31). Oocytes were injected with either 25 ng of mNDCBE cRNA or with H_2O for controls and incubated for 6 days at 18°C in OR3 medium (Leibovitz's L15 medium diluted to approximately 200 mOsm/kg H_2O) supplemented with penicillin and streptomycin. The day of assay, oocytes were incubated for approximately 5 hours in ND96 containing either 0.5% methanol (vehicle) or ND96 containing 0.25 mM HCTZ/0.5% methanol. The pH_i of the oocytes was monitored as the cells were perfused with a solution containing 5% CO_2/33 mM HCO_3^- in the continued presence of HCTZ and/or vehicle. The measurement of pH_i using a H^+-selective microelectrode has been described in detail elsewhere (53). Briefly, each oocyte is placed in a plastic perfusion chamber and impaled with a H^+-selective microelectrode and a KCl-filled reference electrode. The cell is first perfused with ND96 solution until a stable pH_i reading is obtained, then the perfusion system is switched to deliver a 5% CO_2/33 mM HCO_3^-–containing solution. An initial CO_2-induced acid load was followed by a pH_i increase that was converted — using the calculated buffering power of each oocyte — into a measure of "HCO_3^- flux" into the cells. Data are acquired using an FD223 dual-channel differential electrometer and analyzed using in-house software. HCO_3^- influx data (rates of pH_i increase) are converted into HCO_3^- flux (mM/s) using the calculated buffering power of the oocyte (change in pH_i due to entry of CO_2 plus the open-system buffering power due to HCO_3^-).

Statistics. Experimental results are summarized as mean ± SEM. All statistical comparisons were made by use of unpaired Student's *t* test or by ANOVA followed by a Bonferroni's post-hoc test when appropriate. A *P* value less than 0.05 was considered significant.

Acknowledgments

Dominique Eladari and coworkers are funded by the Institut National de La Santé et de la Recherche Médicale (INSERM), by the Transatlantic Network on Hypertension from the Fondation Leducq, and by grant PHYSIO 2007-RPV07084 to D. Eladari from l'Agence Nationale de la Recherche (ANR); Christian A. Huebner and coworkers are funded by the Deutsche Forschungsgemeinschaft (grant HU 800/3-1 and HU 800/2-1 to C.A. Hübner), and Susan Wall is funded by the National Institute of Diabetes and Digestive and Kidney Diseases (grant DK 52935).

Received for publication June 10, 2009, and accepted in revised form February 3, 2010.

Address correspondence to: Dominique Eladari, INSERM U872, Equipe 3, 15 rue de l'Ecole de Médecine, Esc. E RDC, F-75006, Paris, France. Phone: 33.144413718; Fax: 33.144413717; E-mail: dominique.eladari@crc.jussieu.fr.

Hassan Hatim's present address is: University of Chicago, Section of Nephrology, Department of Medicine, Chicago, Illinois, USA.

1. Guyton AC. Blood pressure control — special role of the kidneys and body fluids. *Science*. 1991; 252(5014):1813–1816.
2. Tse CM, Brant SR, Walker MS, Pouyssegur J, Donowitz M. Cloning and sequencing of a rabbit cDNA encoding an intestinal and kidney-specific Na+/H+ exchanger isoform (NHE-3). *J Biol Chem*. 1992; 267(13):9340–9346.
3. Gamba G, et al. Molecular cloning, primary structure, and characterization of two members of the mammalian electroneutral sodium-(potassium)-chloride cotransporter family expressed in kidney.

J Biol Chem. 1994;269(26):17713–17722.
4. Gamba G, et al. Primary structure and functional expression of a cDNA encoding the thiazide-sensitive, electroneutral sodium-chloride cotransporter. *Proc Natl Acad Sci U S A*. 1993;90(7):2749–2753.
5. Canessa CM, et al. Amiloride-sensitive epithelial Na+ channel is made of three homologous subunits. *Nature*. 1994;367(6462):463–467.
6. Chang SS, et al. Mutations in subunits of the epithelial sodium channel cause salt wasting with hyperkalaemic acidosis, pseudohypoaldosteronism type 1. *Nat Genet*. 1996;12(3):248–253.
7. Schultheis PJ, et al. Renal and intestinal absorptive defects in mice lacking the NHE3 Na+/H+ exchanger. *Nat Genet*. 1998;19(3):282–285.
8. Simon DB, Karet FE, Hamdan JM, DiPietro A, Sanjad SA, Lifton RP. Bartter's syndrome, hypokalaemic alkalosis with hypercalciuria, is caused by mutations in the Na-K-2Cl cotransporter NKCC2. *Nat Genet*. 1996;13(2):183–188.
9. Simon DB, et al. Gitelman's variant of Bartter's syndrome, inherited hypokalaemic alkalosis, is caused by mutations in the thiazide-sensitive Na-Cl cotransporter. *Nat Genet*. 1996;12(1):24–30.
10. Ji W, et al. Rare independent mutations in renal salt handling genes contribute to blood pressure variation. *Nat Genet*. 2008;40(5):592–599.
11. Lifton RP, Gharavi AG, Geller DS. Molecular mechanisms of human hypertension. *Cell*. 2001; 104(4):545–556.
12. Beyer KH Jr, Baer JE, Russo HF, Noll R. Electrolyte excretion as influenced by chlorothiazide. *Science*. 1958;127(3290):146–147.
13. Chobanian AV, et al. The seventh report of the joint national committee on prevention, detection, evaluation, and treatment of high blood pressure: the JNC 7 report. *JAMA*. 2003;289(19):2560–2572.
14. ALLHAT Officers and Coordinators for the ALLHAT Collaborative Research Group. Major outcomes in high-risk hypertensive patients randomized to angiotensin-converting enzyme inhibitor or calcium channel blocker vs diuretic: The Antihypertensive and Lipid-Lowering Treatment to Prevent Heart Attack Trial (ALLHAT). *JAMA*. 2002; 288(23):2981–2997.
15. Velazquez H, Wright FS. Effects of diuretic drugs on Na, Cl, and K transport by rat renal distal tubule. *Am J Physiol*. 1986;250(6 Pt 2):F1013–F1023.
16. Greger R. Physiology of renal sodium transport. *Am J Med Sci*. 2000;319(1):51–62.
17. Terada Y, Knepper MA. Thiazide-sensitive NaCl absorption in rat cortical collecting duct. *Am J Physiol*. 1990;259(3 Pt 2):F519–F528.
18. Tomita K, Pisano JJ, Burg MB, Knepper MA. Effects of vasopressin and bradykinin on anion transport by the rat cortical collecting duct. Evidence for an electroneutral sodium chloride transport pathway. *J Clin Invest*. 1986;77(1):136–141.
19. Tomita K, Pisano JJ, Knepper MA. Control of sodium and potassium transport in the cortical collecting duct of the rat. Effects of bradykinin, vasopressin, and deoxycorticosterone. *J Clin Invest*. 1985; 76(1):132–136.
20. Pech V, Kim YH, Weinstein AM, Everett LA, Pham TD, Wall SM. Angiotensin II increases chloride absorption in the cortical collecting duct in mice through a pendrin-dependent mechanism. *Am J Physiol Renal Physiol*. 2007;292(3):F914–F920.
21. Garty H, Palmer LG. Epithelial sodium channels: function, structure, and regulation. *Physiol Rev*. 1997; 77(2):359–396.
22. Rubera I, et al. Collecting duct-specific gene inactivation of alphaENaC in the mouse kidney does not impair sodium and potassium balance. *J Clin Invest*. 2003;112(4):554–565.
23. Schultheis PJ, et al. Phenotype resembling Gitelman's syndrome in mice lacking the apical Na+-Cl– cotransporter of the distal convoluted tubule. *J Biol Chem*. 1998;273(44):29150–29155.
24. Brooks HL, et al. Profiling of renal tubule Na+ transporter abundances in NHE3 and NCC null mice using targeted proteomics. *J Physiol*. 2001; 530(Pt 3):359–366.
25. Loffing J, et al. Altered renal distal tubule structure and renal Na(+) and Ca(2+) handling in a mouse model for Gitelman's syndrome. *J Am Soc Nephrol*. 2004;15(9):2276–2288.
26. Wall SM, et al. NaCl restriction upregulates renal Slc26a4 through subcellular redistribution: role in Cl- conservation. *Hypertension*. 2004;44(6):982–987.
27. Royaux IE, et al. Pendrin, encoded by the Pendred syndrome gene, resides in the apical region of renal intercalated cells and mediates bicarbonate secretion. *Proc Natl Acad Sci U S A*. 2001;98(7):4221–4226.
28. LeHir M, Kaissling B, Koeppen BM, Wade JB. Binding of peanut lectin to specific epithelial cell types in kidney. *Am J Physiol*. 1982;242(1):C117–C120.
29. Weiner ID, Hamm LL. Use of fluorescent dye BCECF to measure intracellular pH in cortical collecting tubule. *Am J Physiol*. 1989;256(5 Pt 2):F957–F964.
30. Parker MD, Musa-Aziz R, Rojas JD, Choi I, Daly CM, Boron WF. Characterization of human SLC4A10 as an electroneutral Na/HCO3 cotransporter (NBCn2) with Cl- self-exchange activity. *J Biol Chem*. 2008; 283(19):12777–12788.
31. Grichtchenko II, et al. Cloning, characterization, and chromosomal mapping of a human electroneutral Na(+)-driven Cl-HCO3 exchanger. *J Biol Chem*. 2001;276(11):8358–8363.
32. Beyer KH, Baer JE. Physiological basis for the action of newer diuretic agents. *Pharmacol Rev*. 1961; 13:517–562.
33. Boedtkjer E, Praetorius J, Fuchtbauer EM, Aalkjaer C. Antibody-independent localization of the electroneutral Na+-HCO3– cotransporter NBCn1 (slc4a7) in mice. *Am J Physiol Cell Physiol*. 2008; 294(2):C591–C603.
34. Pushkin A, et al. NBC3 expression in rabbit collecting duct: colocalization with vacuolar H+-ATPase. *Am J Physiol*. 1999;277(6 Pt 2):F974–F981.
35. Loffing J, Kaissling B. Sodium and calcium transport pathways along the mammalian distal nephron: from rabbit to human. *Am J Physiol Renal Physiol*. 2003;284(4):F628–F643.
36. Bachmann S, Velazquez H, Obermuller N, Reilly RF, Moser D, Ellison DH. Expression of the thiazide-sensitive Na-Cl cotransporter by rabbit distal convoluted tubule cells. *J Clin Invest*. 1995;96(5):2510–2514.
37. Obermuller N, et al. Expression of the thiazide-sensitive Na-Cl cotransporter in rat and human kidney. *Am J Physiol*. 1995;269(6 Pt 2):F900–F910.
38. Loffing J, et al. Distribution of transcellular calcium and sodium transport pathways along mouse distal nephron. *Am J Physiol Renal Physiol*. 2001; 281(6):F1021–F1027.
39. Plotkin MD, et al. Localization of the thiazide sensitive Na-Cl cotransporter, rTSC1 in the rat kidney. *Kidney Int*. 1996;50(1):174–183.
40. Pradervand S, et al. Salt restriction induces pseudohypoaldosteronism type 1 in mice expressing low levels of the beta-subunit of the amiloride-sensitive epithelial sodium channel. *Proc Natl Acad Sci U S A*. 1999;96(4):1732–1737.
41. Meneton P, Loffing J, Warnock DG. Sodium and potassium handling by the aldosterone-sensitive distal nephron: the pivotal role of the distal and connecting tubule. *Am J Physiol Renal Physiol*. 2004; 287(4):F593–F601.
42. Coffman TM. A WNK in the kidney controls blood pressure. *Nat Genet*. 2006;38(10):1105–1106.
43. Kahle KT, et al. WNK4 regulates the balance between renal NaCl reabsorption and K+ secretion. *Nat Genet*. 2003;35(4):372–376.
44. Lalioti MD, et al. Wnk4 controls blood pressure and potassium homeostasis via regulation of mass and activity of the distal convoluted tubule. *Nat Genet*. 2006;38(10):1124–1132.
45. Morris RG, Hoorn EJ, Knepper MA. Hypokalemia in a mouse model of Gitelman's syndrome. *Am J Physiol Renal Physiol*. 2006;290(6):F1416–F1420.
46. Jacobs S, et al. Mice with targeted Slc4a10 gene disruption have small brain ventricles and show reduced neuronal excitability. *Proc Natl Acad Sci U S A*. 2008; 105(1):311–316.
47. Burg M, Grantham J, Abramow M, Orloff J. Preparation and study of fragments of single rabbit nephrons. *Am J Physiol*. 1966;210(6):1293–1298.
48. Bourgeois S, Masse S, Paillard M, Houillier P. Basolateral membrane Cl(-)-, Na(+)-, and K(+)-coupled base transport mechanisms in rat MTALH. *Am J Physiol Renal Physiol*. 2002;282(4):F655–F668.
49. Lerolle N, Bourgeois S, Leviel F, Lebrun G, Paillard M, Houillier P. Angiotensin II inhibits NaCl absorption in the rat medullary thick ascending limb. *Am J Physiol Renal Physiol*. 2004;287(3):F404–F410.
50. Di Stefano A, Jounier S, Wittner M. Evidence supporting a role for KCl cotransporter in the thick ascending limb of Henle's loop. *Kidney Int*. 2001; 60(5):1809–1823.
51. Ramsay JA, Brown RHJ, Croghan PC. Electrometric titration of chloride in small volumes. *J Exp Biol*. 1955; 32:822–829.
52. Knauf F, Yang CL, Thomson RB, Mentone SA, Giebisch G, Aronson PS. Identification of a chloride-formate exchanger expressed on the brush border membrane of renal proximal tubule cells. *Proc Natl Acad Sci U S A*. 2001;98(16):9425–9430.
53. Toye AM, et al. The human NBCe1-A mutant R881C, associated with proximal renal tubular acidosis, retains function but is mistargeted in polarized renal epithelia. *Am J Physiol Cell Physiol*. 2006; 291(4):C788–C801.